

Single-channel lunar scintillometer

A. Tokovinin, E. Bustos

Version 2. Sep 11, 2006 [lusci2.tex]

1 The aim of the experiment

Scintillation of the Moon provides a relatively simple method to evaluate the intensity of turbulence in the surface layer (up to few tens of meters above ground). A multi-channel instrument based on the spatial analysis is being developed at the Vancouver University by Paul Hickson and Arlin Crotts. We study here the feasibility of a simple one-channel scintillometer.

2 Principle of operation

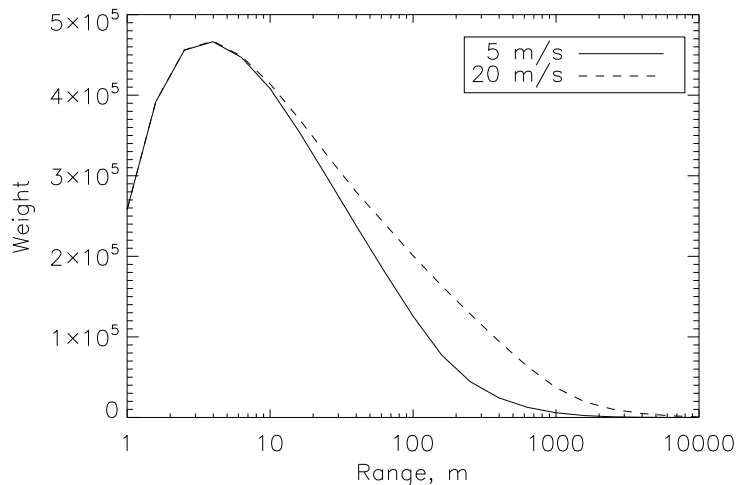


Figure 1: Weighting function of a scintillometer with round aperture of 1.13 cm diameter observing full Moon, with a high-pass signal filtering above 1 Hz. The two curves correspond to the wind speeds of 5 and 20 m/s.

Figure 1 shows the weighting function – scintillation index $\sigma_I^2 = \langle \Delta I^2 \rangle / \langle I \rangle$ produced by a single turbulent layer with unit turbulence integral $J = C_n^2 dh$. The WF is measured in $\text{m}^{-1/3}$. Suppose that a single layer is located at a distance of 2-10 m, near the maximum of the WF where it is equal to $W \approx 4.5 \cdot 10^5$, and it produces a measured scintillation index σ_I^2 . The seeing ϵ (in arcseconds) caused by this layer is computed as

$$\epsilon = [\sigma_I^2 / (W \times 6.8 \cdot 10^{-13})]^{0.6} \quad (1)$$

because $J = 6.8 \cdot 10^{-13}$ corresponds to $\epsilon = 1''$.

In fact turbulence is distributed at all altitudes. For the same integral J , the scintillation will be less because the weighting function is not at its maximum. By still using the formula (1), we will obtain a seeing estimate smaller than the true seeing. Thus the scintillometer provides *a lower bound of the seeing produced by the surface layer*. Considering that turbulence is most intensive near the maximum of the WF, we expect that this measurement will often be close to the actual SL seeing.

3 The instrument

Our first idea was to use a piece of the solar panel as a large (5 cm diameter) light detector. However, it was found by experiment that this detector has a strange temporal response (it amplifies high frequencies), low sensitivity and large noise. We use a large-area Si photo-diode FDS1010 from Thor Labs (www.thorlabs.com). It has a 1 cm^2 square sensitive area. The responsivity is around 0.65 A/W at 900 nm, with NEP of $5.5 \times 10^{-14} \text{ W}/\sqrt{\text{Hz}}$ at this wavelength.

The photo-diode is used with zero bias voltage. The first amplifier is a trans-impedance stage based on the low-noise amplifier OPA627 (Burr-Brown). The feedback resistances are 100K, 1M, 10M (gain range 100x) with capacitors 1.6nF, 160pF and 16pF respectively which restrict the bandwidth. We checked the temporal response by illuminating the sensor with a LED powered by the pulse generator and saw the expected impulse response (which was not the case for the solar-panel detector). These measurements were done with the help of M. Warner.

The second amplifier stage is connected through the 0.1 Hz high-pass filter and amplifies the AC part of the signal by 100 times, also filtering it below 1kHz. The amplification coefficient has been checked by recording the signal from an incandescent lamp, modulated at 100 Hz with an amplitude of 4%. The rms amplitude of the 100-Hz signal in DC and AC channels was 43.1 mV and 4.19 V, giving an amplification factor $k = 97$.

The amplifiers are powered by a DC/DC converter TEN 4-2423 from TRACO Power (9V to $\pm 15 \text{ V}$). The internal frequency of this converter (around 350 kHz) may leak into the output signal, despite filtering and shielding.

The DC and AC signals from the two amplifiers are fed to the analog-digital converter UDAQ 1616DA from CyberResearch. This is a multi-channel data acquisition module with USB interface. We use channels 0 (AC) and 1 (DC) in differential mode. The AC input is additionally filtered by a pair of 0.5K resistors and a $0.5 \mu\text{F}$ capacitor, to remove any pick-up of radio-frequency noise and the fast noise from the amplifiers. The signal ground of the converter is connected through the cable's shield with the amplifier's ground. There seem to be some electrical connection with the laptop computer through the USB cable: we observe different levels of the power-line leakage into the signal depending on the type of the laptop and its power supply (battery or AC). In some cases, there is no leakage.

4 Software

The standard software provided by CyberResearch has basic functions for examining the signals and their spectra. This software is useful for the initial de-bugging of the system. The prototype data acquisition software has been written by E. Bustos in C language. It captures the signals at 1 kHz sampling rate. In fact the UDAQ channels are sampled sequentially, so the actual sampling rate is 2 kHz. After some experiments, we increased the sampling to 20 kHz and recorded average values of 10 samples, leading to the same sampling rate of 1 kHz per channel with additional low-pass filtering.

The data are recorded in ASCII files named after UT moment of the acquisition start, e.g. '2ch_2006-09-08_0117.dat'. Each second of data is recorded separately as pairs of (Ch0, Ch1) ADU counts, preceded with a comment line that shows the acquisition time and other parameters.

The data can be read by the IDL code `rd2cha.pro`. Then the procedure `power` calculates the average value, variance and power spectrum of each channel. The scintillation index is computed as a square ratio of the variance in channel 0 (AC) to the average DC level, taking into account the AC amplification:

$$\sigma_I^2 = [\sigma_{AC}/(DC \times k)]^2. \quad (2)$$

The minimum seeing is then calculated from Eq. 1 with $W = 4.5 \cdot 10^5$. So far, no correction for the air mass or Moon phase is done.

The procedure `treat` combines reading the data and power-spectrum processing. For the purpose of this study, the variance and scintillation index were computed only in the frequency band from 1 Hz (1-s data segments) to 55 Hz (to avoid the 60 Hz pickup). The procedure `model` in the same file compares the observed power spectra with the models (see below).

5 System response and noise

Response. The response of a Si photo-diode is well known, as well as the Moon's flux. Calculation by P. Hickson indicates that a 1 cm^2 detector should produce a photo-current of 100 nA. In our tests a current of 86 nA was measured from the full Moon seen at a large air mass. Assuming the current $i = 90 \text{ nA}$, the detected photon flux is $N = i/1.602 \cdot 10^{-19} = 5.5 \cdot 10^{11} \text{ phe/s}$.

Noise. The *shot noise* of the photo-current in $\tau = 1 \text{ ms}$ integration time corresponds to the relative signal variation of $\sigma_I = (N\tau)^{-1/2} = 4.24 \cdot 10^{-5}$, or a scintillation index $\sigma_I^2 = 1.80 \cdot 10^{-9}$. The rms voltage fluctuations in the AC channel are then $k \sigma_I \times 900 \text{ mV} = 3.8 \text{ mV}$. In the 50 Hz bandwidth the shot noise will be $\sqrt{20}$ times smaller, or 0.85 mV.

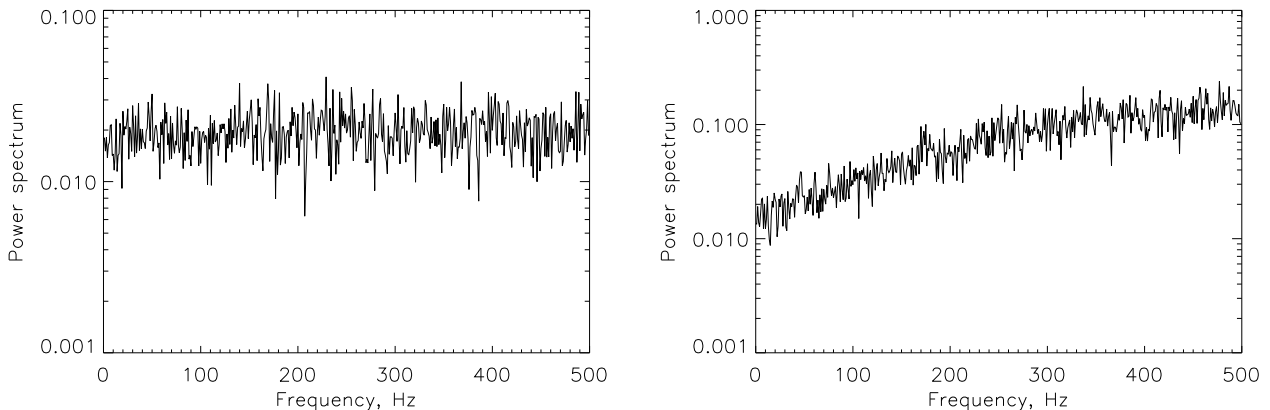


Figure 2: Power spectra (in arbitrary units) of the dark signal without the photo-diode (left) and with it (right) measured on Sept. 11, 2006 in the office with A.Tokovinin's laptop. There is no pick-up signal at 50 Hz.

The noise of the amplifier is dominated by the *Johnson noise* of the load resistor $R = 10\text{M}$. The data sheet of the amplifier manufacturer gives for such a resistance the voltage noise of $400 \text{ nV}/\sqrt{\text{Hz}}$

(P.Hickson obtained the same number by direct calculation). In a 1 kHz bandwidth the noise should be $12.6 \mu\text{V}$ rms, or 1.3 mV at the AC output (amplification $k = 100$). In the 50 Hz bandwidth the expected noise is 0.28 mV.

The internal *noise of the photo-diode* is specified as $\text{NEP} = 5.5 \cdot 10^{-14} \text{ W} \sqrt{\text{Hz}}$ at 900 nm wavelength (0.65 A/W), or 0.25 mV at the AC output with our 10M load resistor and 50 Hz bandwidth. This is less than the Johnson noise. Both noise sources appear to be inferior to the shot noise of the Moon’s signal itself.

We actually measure in the 50 Hz bandwidth the rms noise of 0.45 mv, with the photo-diode either connected or disconnected. The noise in the full 1 kHz bandwidth is 2.7 mV with the diode and 1.44 mV without. The difference (Fig. 2) is due to the additional high-frequency power which appears when the photo-diode is connected. This could be caused by the diode’s capacity. These measurements were taken with a 10-fold averaging of the DAC readings, otherwise the noise level is higher.

The diode’s maximum dark current is specified as 600 nA – much larger than the actual signal from the Moon. This dark signal refers to the nominal photo-diode operation with -5 V bias. We operate without bias and do not detect any significant dark current. A biased operation may make things worse by increasing the dark current and its shot noise (to be tested).

6 Scintillometer test on September 7, 2006

On September 7, 2006, E. Bustos, A. Tokovinin and J. Rajagopal brought the equipment to Cerro Tololo for tests. The Moon was nearly full, low above the horizon (air mass XXX). The sky was clear, with a very slow wind estimated as $\sim 0.5 \text{ m/s}$ (the meteo service measured 1.9 mph speed).

As noted, the DC signal from the Moon was about 860 mV. The baffle around the detector admitted a large portion of the sky (angle about 20°). Yet, by shadowing the moon we did not measure any signal at all and estimated that the sky background was less than 2% of the Moon’s signal.

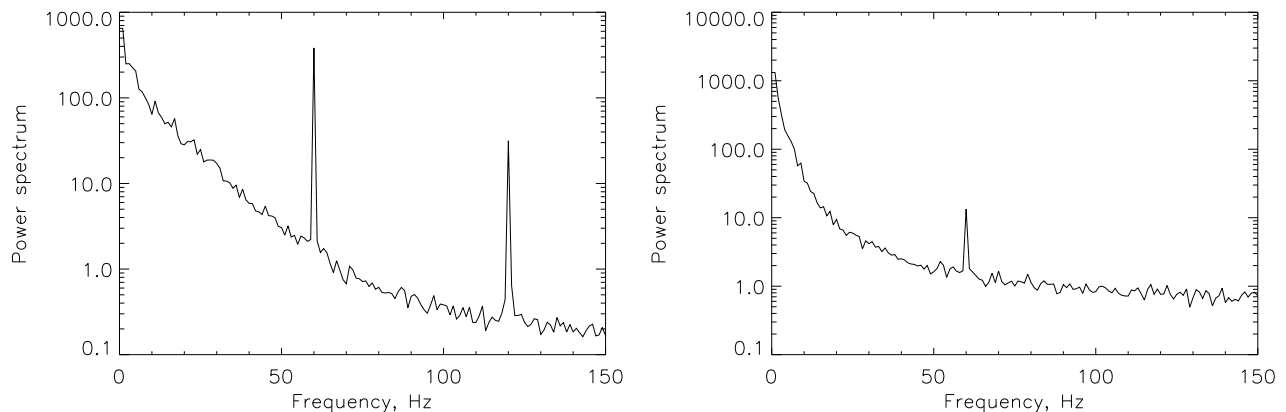


Figure 3: Low-frequency portions of two power spectra (in arbitrary units) of the Moon recorded on Sept. 7, 2006. The spectrum on the left was taken at 01:25 with the new software (fast sampling and averaging) and the laptop of E.Bustos on battery power. The spectrum on the right was taken at 01:41 with the old software (1kHz sampling) and the laptop of A.Tokovinin.

The 110V power at Tololo has a frequency of 60 Hz. The pick-up noise at 60 Hz and higher harmonics was variable, depending on the computer and its power. It was strongest with the laptop of E. Bustos powered from 110V. On the other hand, on the laptop of A. Tokovinin, disconnecting the power (i.e. switching to the battery) actually increased the 60 Hz signal, which was quite weak in both cases. (the same combination in the office was free from any pick-up.) The low-frequency portions of two good signal spectra are presented in Fig. 3.

All records (even those with strong pick-up) were successfully processed with the `rd2cha.pro`. The scintillation index was calculated from the power below 55 Hz, and all records gave consistent values. The values of average DC signal and AC rms fluctuations (full bandwidth and below 55 Hz) in mV are listed below, as well as the scintillation indices and minimum seeing in arcseconds calculated by Eq. 1. The UT time refers to the start of each acquisition on Sept. 8, 2006.

UT	Nsec	DC	AC	AC1	Scind	Seeing
01:17	48	821.81	77.68	21.38	6.766	0.404
01:19	60	820.95	76.71	18.06	4.838	0.331
01:23	44	820.23	79.40	27.05	10.873	0.537
01:25	56	819.57	25.63	23.53	8.239	0.455
01:27	60	818.93	30.47	28.70	12.279	0.578
01:28	57	817.10	25.43	23.33	8.153	0.452
01:38	50	861.10	23.16	21.75	6.377	0.390
01:41	60	860.33	22.26	20.76	5.820	0.369
01:43	58	858.87	25.79	24.47	8.115	0.451
01:46	41	-11.10	7.13	2.21	dark	
01:47	35	-11.55	7.05	2.17	dark	
01:49	49	858.74	24.62	23.28	7.349	0.425
01:50	56	857.80	28.74	27.00	9.905	0.508

We see from Fig. 3 that the new software gave a lower noise floor. Indeed, the two measurements of the noise made with the old code (see the Table) are higher than the measurements repeated later with the new code.

7 Analysis

The lunar SHABAR of P Hickson was working during our tests. The SHABAR acquisition which started on 01:19 (overlapping with our data) has given the scintillation index of 7.2 and the first covariance at 1.8 cm baseline of 6.2 (in units of 1E-8). The SHABAR has smaller detectors and is sensitive to closer turbulence. Both instruments measured rather good seeing in the surface layer. It is not possible to compare the seeing quantitatively because our processing is still rudimentary (no airmass correction). More simultaneous data are needed.

During the period of our measurements, the Tololo DIMM measured a seeing degrading from 1.2'' to 1.5''. Unfortunately, the MASS was not operational for some reason and we cannot deduce the integrated seeing in the ground layer.

The scintillometer signal is produced by turbulence distributed at different ranges. Yet, it is instructive to compare the observed power spectra with the models for a single layer. We place this fiducial layer at 10 m distance (near the maximum of our sensitivity curve), suppose that it produces

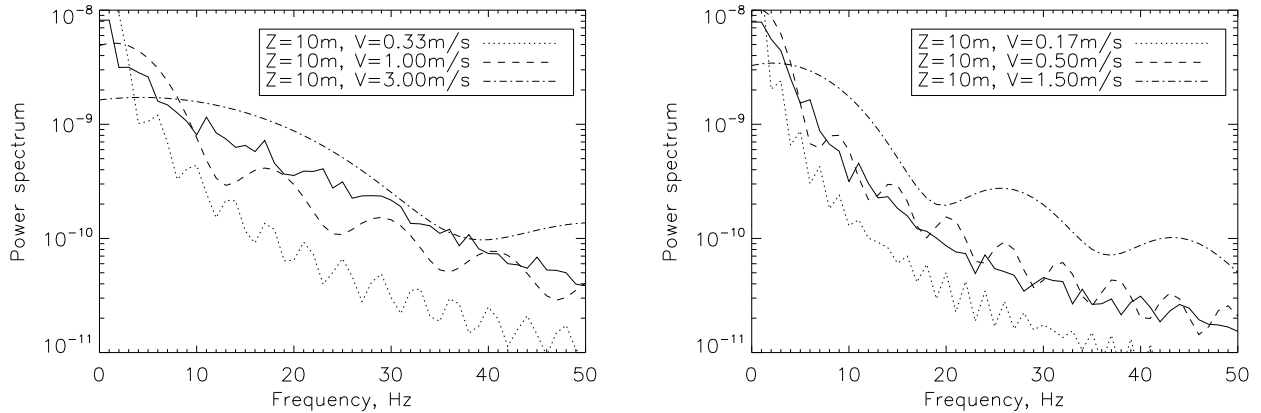


Figure 4: Power spectra from Fig. 3 with different normalization (full lines) and the models of a single turbulent layer at 10 m range moving with different speeds.

the 0.3'' seeing, and try different wind speeds. The results in Fig. 4 demonstrate a good qualitative agreement with the measured the spectra. The change of the wind speed by 3 times is easily detectable and permits to reject wrong models.

A similar set of models for a layer at 20 m distance can be fitted, but it calls for a larger wind speed in order to reach an agreement. Thus, we confirm the known result that the spectrum essentially depends on the characteristic frequency $\nu_0 = V/d_e$, where the effective averaging diameter $d_e = \sqrt{d^2 + (\theta z)^2}$. When the wind speed is known, we can deduce the thickness of the surface layer from the known ν_0 or, better, invert the spectrum and compute the C_n^2 profile in the SL.

8 Conclusions

We demonstrated the technical feasibility of measuring the scintillation of Moon. A fairly simple device reaches the sensitivity limited essentially by the photon noise. The sky background is not significant, permitting to use a wide baffle and to operate without tracking the Moon. The temporal spectrum of the scintillation and its overall power are in reasonable agreement with models.

A method of inverting the profile from signals of one or several photo-diodes will be developed and studied by simulations. This will lead to the definition of a simple instrument for SL turbulence measurement. Our prototype hardware provides a basis for such development.